Polypropylene/Combinational Inorganic Filler Micro-/Nanocomposites: Synergistic Effects of Micro-/Nanoscale Combinational Inorganic Fillers on Their Mechanical Properties

Deliang Chen,[1] Huaming Yang[2]

[1]*School of Materials Science and Engineering, Zhengzhou University, Zhengzhou 450001, People's Republic of China*
[2]*Department of Inorganic Materials, School of Resources Processing and Bioengineering, Central South University, Changsha 410083, People's Republic of China*

Received 19 February 2009; accepted 11 July 2009
DOI 10.1002/app.31104
Published online 8 September 2009 in Wiley InterScience (www.interscience.wiley.com).

ABSTRACT: Polypropylene (PP) has wide applications in various areas, but its low-temperature brittleness and low moduli have limited its applications in engineering areas. This article reported micro-/nanoscale combinational inorganic fillers (CIFs) to reinforce PP-matrix composites as the first example. The CIFs consisted of plate-like talc (T), needle-like wollastonite (W), and nano-Al_2O_3 (N). The PP/CIFs specimens were fabricated via a process of twin-screw extrusion and screw-type injection molding. The mechanical properties and thermal deflection temperature (HDT) of the PP/CIF composites were tested according to the corresponding standards, and the morphologies of the tensile-fractured sections were observed using FE-SEM. The PP/WT composites had higher mechanical properties and HDTs than those of either PP/W or PP/T. Small amounts of Al_2O_3 nanocrystals together with WT simultaneously strengthened and toughened the PP-matrix composites. The PP/WTN composite with 2.6% of nano-Al_2O_3 had well-balanced properties, enhanced by a large increment when compared with the PP matrix or PP/WT composites. The enhancements should be attributed to the synergistic effects of the CIFs not only in the aspect of various shapes (plate-like, needle-like, and spherical) but also in hierarchical size-levels (microscale and nanoscale). The novel strategy overcame the limitation of conventional rigid modification and solved the problem of uniform dispersion of nanocrystals in polymer matrices. © 2009 Wiley Periodicals, Inc. J Appl Polym Sci 115: 624–634, 2010

Key words: poly(propylene)(PP); nanocomposites; reinforcement; mechanical properties; fillers

INTRODUCTION

Polymer-matrix composites have attracted increasing attention not only in the scientific aspects but also in their engineering applications, because of their unique performances of high-specific strengths, excellent processability, and various functionalities.[1–4] Polypropylene (PP), one of the most important general-purpose thermoplastics, is of well-balanced physico-chemical and mechanical properties, having various applications in tubing, cable, automobile, housing, electronics, and electrical industries.[5,6] Some drawbacks, however, such as low-temperature brittleness, low modulus, and large shrinkage ratios have limited its applications in high-performance engineering areas.[7–10] To overcome these limitations, scientists have developed a number of methods to modify PP-matrix composites.[11–14] Microsized inorganic fillers, including talc, wollastonite, calcium carbonate, barium sulfate, carbon black, magnesium hydroxide, hydroxyapatite, glass beads, montmorillonite, and aluminum, have been applied not only to lower the material costs but also to enhance the moduli and toughnesses of PP-matrix materials and reduce their shrinkage rates of forming.[6,13,15–23] The addition of microsized inorganic fillers usually damages the tensile and/or flexural strength of PP-matrix composites.[23,24] Modification of PP with organic elastomers is an effective way to improve the toughnesses of PP-matrix materials, but their moduli usually decrease obviously.[25–27] To reach a good balance between strengths, moduli, and toughnesses, scientists have designed polynary systems (*i.e.*, nano-$CaCO_3$/SBS/PP, PP/POE/$BaSO_4$, PP/EOR/$CaCO_3$, PP/EPDM/nano-$CaCO_3$, and PP/SEBS-*g*-MA/wollastonite), consisting both of inorganic fillers and of organic elastomers to reinforce PP-matrix

Correspondence to: D. L. Chen (dlchen@zzu.edu.cn) or H. M. Yang (hmyang@csu.edu.cn).
Contract grant sponsor: National Natural Science Foundation of China; contract grant number: 50802090.
Contract grant sponsor: Introduced Talent Project of Zhengzhou University.

materials.[28–32] One should note that such polynary systems are complex and expensive in material preparation. Cellulose fibers and wood flours have also been used to modify PP materials.[9,11,33–37] Nanocrystalline inorganic fillers (*i.e.*, carbon nanotubes, nano-SiO_2, nano-$CaCO_3$, and organoclays) have been extensively investigated to modify polymers, and a number of reports indicate that small amounts of nanocrystalline fillers can strengthen, toughen, and functionalize PP-matrix materials.[2,14,32,38–48] But there are two big challenges in reinforcing polymer-matrix materials with nanocrystalline fillers: one is the uniform dispersion of nanocrystals in polymer matrix and the other is the high costs.[39,49] To the best of our knowledge, there have been no efficient routes to solve these problems yet.

For multicomponent composites, the factors that influence their properties are very complicated.[46,50] Interfacial adhesion of various components is one of the most important factors, and an adequate adhesion strength is vital to mechanical properties of polymer composites.[28,29,45-47] Coupling agents, compatibilizers, and irradiation grafting polymerization have been usually used to modify the surfaces of inorganic fillers and consequently to enhance the affinity and bonding strength between inorganic fillers and organic matrices.[11,18,23,33,34,38–49] Particle sizes and morphologies of inorganic fillers are also found to be important factors that influence the properties of polymer composites.[20–24,31,32,41,42,50,51] In addition, uniform dispersion of the filler particles in polymer matrices has been a precondition of achieving an effective reinforcement.[39] On the basis of the literature survey, inorganic fillers with singular species are widely used to reinforce polymer-matrix composites,[13–24,40–46] whereas the combinational inorganic fillers (CIFs), consisting of various species of particles with different morphologies and different size-distributions, have seldom been designed to modify polymer composites.[50–54]

This article reports a novel route for strengthening and toughening PP-matrix composites with a series of CIFs composed of ultrafine plate-like talc powders, needle-like wollastonite powders, and spherical Al_2O_3 nanocrystals (Scheme 1). The core of the route proposed here is the utilization of the synergistic effects of CIFs with different shapes and the synergistic effects of CIFs with microscale and nanoscale size-distributions. One objective of this work is to seek a robust and cost-effective process to achieve a simultaneous enhancement in strength and toughness of PP-matrix composites. The other is to develop an effective way to utilize nanocrystals in polymer matrices and to overcome their limitation of aggregation tendency. The analysis of synergistic effects is made on the basis of comparing typical mechanical properties and thermal deflection temperature (HDTs) of the PP/CIF composites with others. The related mechanisms are also discussed according to the SEM observations of tensile-fractured surfaces and dynamic viscosities of the corresponding melts.

EXPERIMENTAL

Materials

Polypropylene (MFI = 2.5 g/10 min, ρ = 0.91 g/cm^3, grade F401), was provided by Luoyang Polypropylene (Luoyang, China). Talc ($Mg_3(Si_4O_{10})(OH)_2$) powders ($\rho = \sim 2.7$ g/cm^3, 5–50 μm in size) were supplied by Guilin Guiguang Talc Co., Ltd. (Guilin, China). Wollastonite ($CaSiO_3$) powders ($\rho = \sim 2.8$ g/cm^3, 50–200 μm in size) were supplied by Gold-Copper Mining (Huangshi, China). Al_2O_3 nanocrystals (10–15 nm in size) were kindly supplied by Guangzhou Institute of Chemistry, CAS (Guangzhou China). The coupling agents of γ-aminopropyltriethoxysilane, (KH-550) and isopropyl-tri(-dioctylpyrophosphate) titanate (NDZ-201) were purchased from Nanjing Shuguang Chemical Group (Nanjing, China). Absolute ethylalcohol (analytical purity) was purchased from Changsha Debo Chemical Co., Ltd. (Changsha, China).

Ultrafine processing of talc and wollastonite powders

Ultrafine processing of the as-received talc and wollastonite powders were conducted in a periodical stirring ball mill (ZJM-20, China), equipped with a columned vessel (useful volume of 4.8 L) and a water cooling system. Zirconia balls (5 mm in diameter) were used as milling media. Talc, wollastonite, and the mixture of talc/wollastonite (mass ratio of 1 : 1) were ground using a dry process, respectively. Typically, 1.0 kg of talc powders for milling and 4.0 kg of zirconia balls were loaded into the vessel and milled for 2.0 h at room temperature. Wollastonite and talc/wollastonite powders were ground under a similar condition.

Surface modification of inorganic fillers

Surface modification of the ultrafine powders was carried out in a high-speed mixer (GH-25, China) with a volume of 25 L, equipped with a stepless-change electric engine (0–1600 rpm) and with an automatic temperature-control system (0–300°C). A mixed coupling agent of KH-550 and NDZ-201 with a mass ratio of 1 : 1 was used as the surface modification agent. For improving the modification effect, the coupling agent was diluted with absolute ethylalcohol before use. Typically, 1.0 kg of the ultrafine

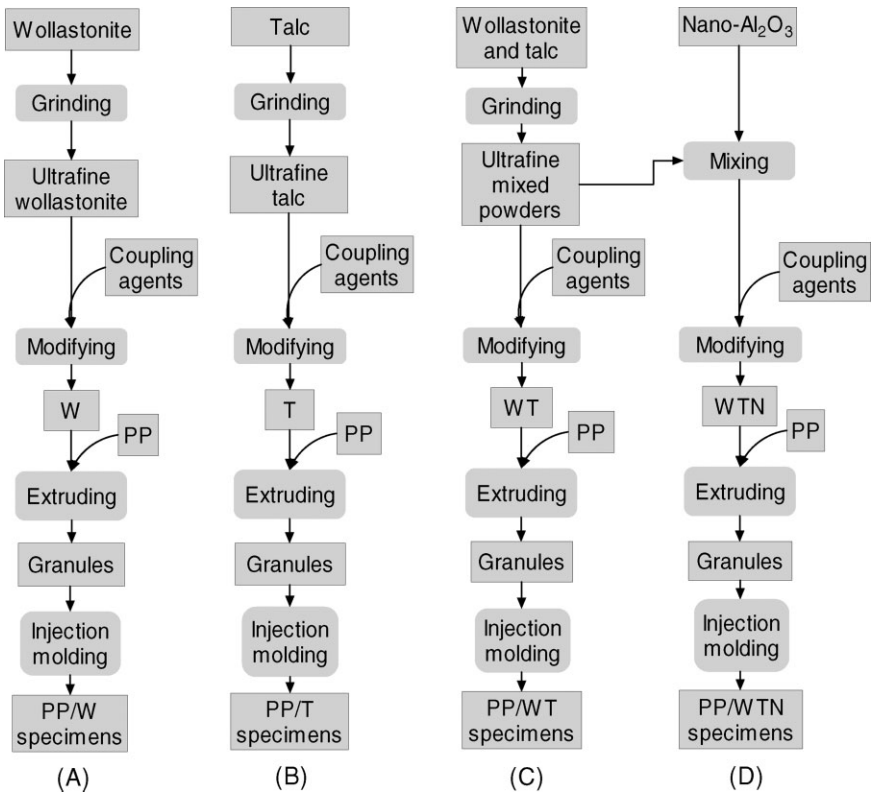

Scheme 1 A Flowchart for the fabrication of PP/CIF micro-/nanocomposites: (a) PP/W, (b) PP/T, (c) PP/WT, and (d) PP/WTN.

talc powders were loaded into the vessel of the high-speed mixer, heating to 80–100°C and mixing at a speed of 1200 rpm for 30 min. At the same time, 5.0 g of KH-550, 5.0 g of NDZ-201, and 50 mL of absolute ethylalcohol were mixed in a dried beaker (200 mL) to form a transparent solution. Then, the diluted coupling agent was added drop by drop into the talc powders using a syringe under a high-speed stirring and heating condition. The stirring and heating was kept for another 30 min after finishing the addition of the coupling agent to evaporate the solvent of ethylalcohol. The modification of wollastonite and talc/wollastonite mixed powders was carried out under a similar condition. For simplicity, the talc, wollastonite, and talc/wollastonite (1 : 1) powders with ultrafine processing and surface modification were denoted as T, W, and WT, respectively. For modification of micro-/nanocomposite powders, Al_2O_3 nanocrystals with a given amount were mixed with the ultrafine talc/wollastonite (1 : 1 in mass) powders under a high-speed stirring and heating condition before the coupling agent was added. Other operating parameters were similar to those for the modification of T, W, and WT. For simplicity, the modified micro-/nanocomposite powders with WT-to-Al_2O_3 mass ratios of 100 : 1, 100 : 3, 100 : 5, and 100 : 8 were denoted as WTN-1, WTN-3, WTN-5, and WTN-8, respectively, and the fillers of WT and WTN with different fractions of nano-Al_2O_3 were called CIFs.

Fabrication of PP/CIF composites

Scheme 1 shows a flowchart for the preparation of PP/CIF composites. Various fractions (0–60 mass%) of inorganic fillers (W, T, WT, and WTN) and PP resin were mixed using a mixer (GH-20, Liaoning, China), and the mixtures were interfused using a twin-screw extruder (PCM-30, Ikegai Tekko Japan) with a length/diameter ratio of 31. The speed was 120 rpm and the barrel temperature was 190– 210°C. The extruded composites were cooled in a water bath, and the cooled composites were then granulated into short rods with sizes less than 3 mm before drying at 80°C for 24 h. The dried granules were injection-molded into multipurpose test specimens according to ISO 3167 using a screw-type injection molding machine (Boy 22S, Germany) with a barrel temperature of $\sim$ 210°C under an injection pressure of $\sim$ 35 MPa. The multipurpose test specimens were then processed to three types of test specimens, including tensile specimens (150 mm long dog bone with a center section of 60 mm $\times$ 10 mm $\times$ 4 mm), flexural specimens (60 mm $\times$ 10 mm

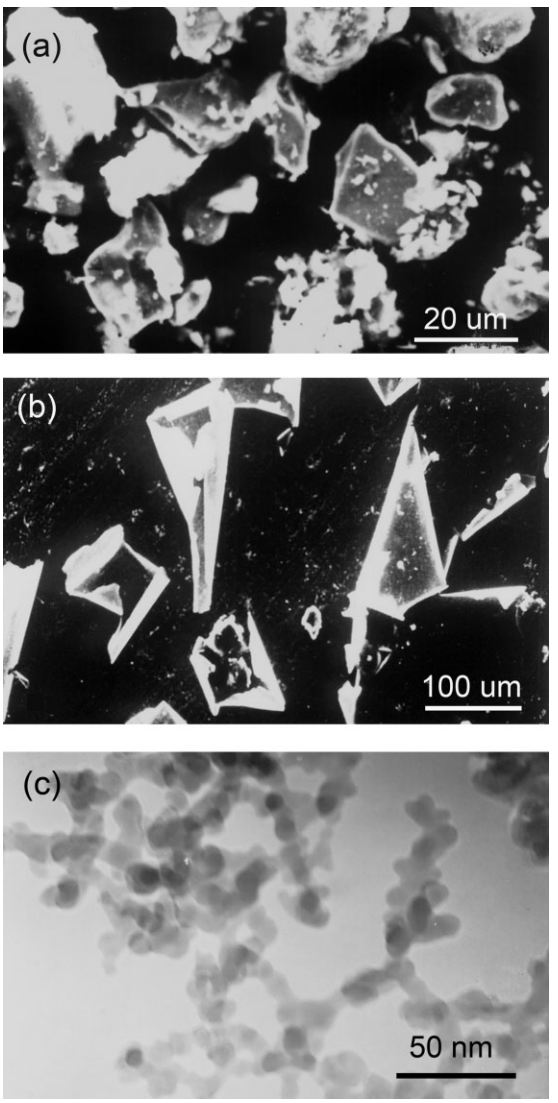

Figure 1 SEM images of (a) talc, (b) wollastonite powders, and (c) TEM image of nano-Al_2O_3 used in PP/CIF composites.

× 4 mm), impact specimens (60 mm × 10 mm × 4 mm) with a notched depth of 0.8 mm, and heat deflection specimens (110 mm × 10 mm × 4 mm).

Characterization techniques

The morphologies of the pristine inorganic powders and the tensile-fractured surfaces of PP/CIF composites were observed using a scanning electron microscope (JSM-6700F). The size and morphology of Al_2O_3 nanocrystals were observed using a transmission electron microscope (JEM-200CX). Particle-size distributions and specific surface areas of the CIFs were measured on a size analyzer (Mastersizer 2000, Malvern, UK). The whitenesses of CIFs were measured using an automatic whiteness meter (WSD-III, China).

An activation exponent (ψ) was introduced to quantitatively evaluate the effects of surface modification. Basically, a given amount (m_{total}) of CIFs were dispersed in water under intense stirring at room temperature for 30 min, and the obtained CIF -water systems were kept still standing for 24 h. The floating CIFs were then collected carefully and dried at 100°C for 2 h. The mass of the dried powders was weighed to be $m_{floating}$. The activation exponent (ψ) was defined as $\Psi = (m_{floating}/m_{total}) \times 100\%$.

The tensile and flexural properties of the PP/CIF composites were measured using an electro-mechanical testing machine (Zwick 1464, Germany) according to the standards of ASTM D638-1999 and ASTM D790-1999, respectively. Five specimens of each sample were tested, and the average values were used to evaluate the properties of the composites. The notched impact strength was measured with an impact tester (XJ-40A, China) according to ASTM D256-1997. The HDT was measured according to the standard of ASTM D648-2000. The viscosities of the PP/CIF melts were measured according to the standard ISO 3219 using a controlled stress rheometer (RS 150, Germany) at 200°C with a frequency of 10 Hz.

RESULTS AND DISCUSSION

Ultrafine processing and surface modification of inorganic fillers

The morphologies of the as-received talc powders, wollastonite powders, and Al_2O_3 nanocrystals were shown in Figure 1. The talc powders exhibit a platelike morphology and their particle size range from 5 to 50 μm [Fig. 1(a)]. The wollastonite powders present a needle-like shape, 200 μm long in length and 50 μm in diameter [Fig. 1(b)]. The TEM image [Fig. 1(c)] of the Al_2O_3 nanocrystals indicates that the Al_2O_3 particles are of a spherical shape with a size range of 10–15 nm and they are well-dispersed. As reinforcements for polymers, the talc, and wollastonite powders are too large in size and they are ground into ultrafine powders. Table I shows the

TABLE I
Physiochemical Properties of Combinational Inorganic Fillers (CIFs) for PP-Matrix Composites

Inorganic fillers	Diameter (D_{50}) (μm)	Specific surface area ($m^2\ g^{-1}$)	Whiteness (%)	Activation exponent (ψ) (%)
W	7.9	1.8	74	~ 94
T	6.2	1.8	89	~ 98
WT	4.3	2.8	85	~ 97
WTN-1	6.0	1.6	84	~ 98
WTN-3	7.1	1.5	84	~ 99
WTN-5	6.2	1.6	84	~ 99
WTN-8	6.2	1.5	85	~ 99

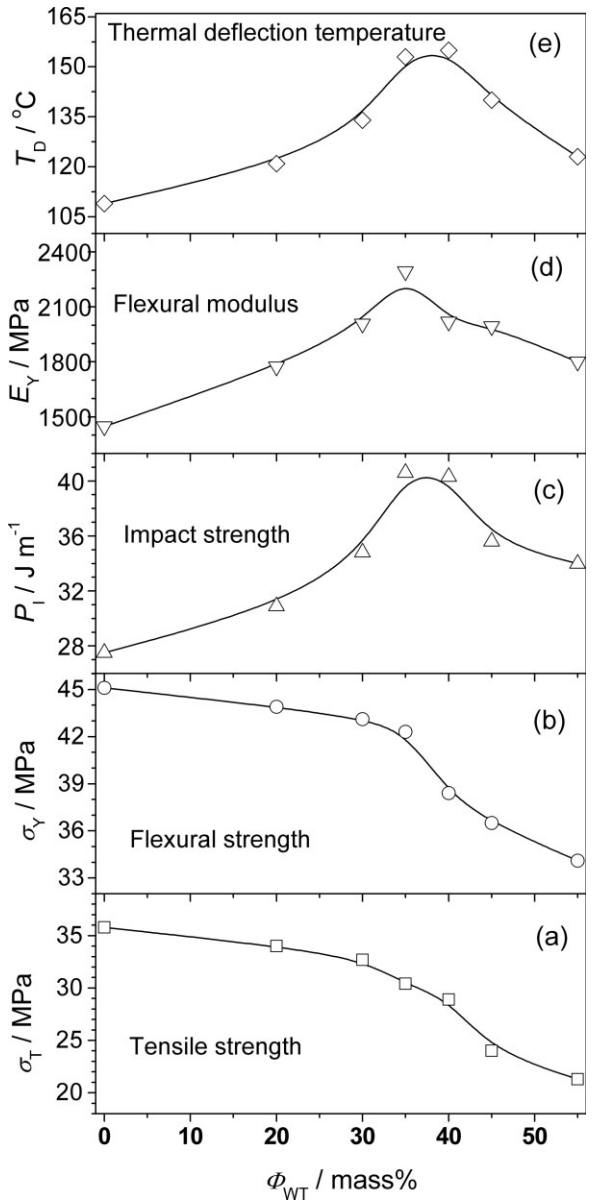

Figure 2 Mechanical properties and thermal deflection temperature of PP/WT composites as a function of the amount of WT.

characteristics of the inorganic fillers after ultrafine processing and surface modification. As Table I shows, the median diameters (D_{50}) of the fillers are 6–8 μm, and their specific surface areas are 1.5–2.8 m^2/g. The whitenesses of the CIFs are larger than 80%. The activation exponents of the fillers modified with a mixed coupling agent of KH-550 and NDZ-201 are larger than 95%.

PP/WT composites: the optimum fraction of inorganic fillers

The combinational filler of WT (1 : 1), consisting of plate-like talc and needle-like wollastonite powders, was firstly used as a typical reinforcement to determine the optimum fraction of inorganic fillers according to the overall mechanical properties of PP/WT composites. Figure 2 shows the typical mechanical properties and HDTs of the PP/WT composites with various fractions (0–55%) of WT. The plot of the tensile strengths (σ_T) of PP/WT composites versus the fractions of WT, as shown in Figure 2(a), indicates that the tensile strength decreases with the increases in WT content (Φ_{WT}). A similar profile is observed for the flexural strength (σ_Y) of PP/WT composites, as shown in Figure 2(b). When the WT amounts are less than 35%, the tensile and flexural strengths of PP/WT composites decrease slightly, whereas their tensile and flexural strengths decrease sharply with a further increase in WT amount [Fig. 2(a,b)].

The notched impact strengths (P_I) increase with increases in the WT content when $\Phi_{WT} \leq 35\%$, and when $\Phi_{WT} > 35\%$, the notched impact strengths of the PP/WT composites decrease sharply, but their values are much larger than that (27.5 J/m) of PP matrix, even when $\Phi_{WT} = 55\%$ [Fig. 2(c)]. The PP/WT composite with 35% WT has the highest notched impact strength (40.6 J/m). The flexural moduli (E_Y) of PP/WT composites show a similar change with increases in the WT content, and the highest flexural modulus (2293 MPa) occurs at $\Phi_{WT} = 35\%$, as shown in Figure 2(d). Figure 2(e) shows the change of the HDTs (T_D) of the PP/WT composites vs. the WT contents. A highest value is observed when $\Phi_{WT} =$ 35–40%, and the HDT of the PP/WT composite increases from 109 to 155°C as the fraction of WT increases from 0 to 40%. When $\Phi_{WT} > 40\%$, the HDT values decrease obviously.

From the changes of mechanical properties and HDTs of PP/WT composites with increases in WT content (0–55%), one can find that when $\Phi_{WT} = 35\%$ the PP/WT composites have well-balanced mechanical properties and HDT: $\sigma_T = 30.4$ MPa, $\sigma_Y = 42.3$ MPa, $E_Y = 2293$ MPa, $P_I = 40.6$ J/m, and $T_D = 153$°C. For convenience in comparing the PP-matrix composites with various inorganic fillers, the filler contents of CIFs are fixed to be 35% for the following PP/CIF composites.

PP/CIFs composites: the effects of various inorganic fillers

Figure 3 shows the mechanical properties and HDTs of the PP-matrix composites with various types of CIFs ($\Phi_{CIF} = 35\%$), including W, T, WT, and WTN-1, respectively. As Figure 3(a) shows, the tensile strengths of PP/W and PP/T are lower than that of PP/WT, and the PP/WTN-1 composite with 0.35% nano-Al_2O_3 has the highest tensile property (34.8 MPa), close to the tensile strength of the PP matrix. The flexural strengths of the PP/CIFs composites

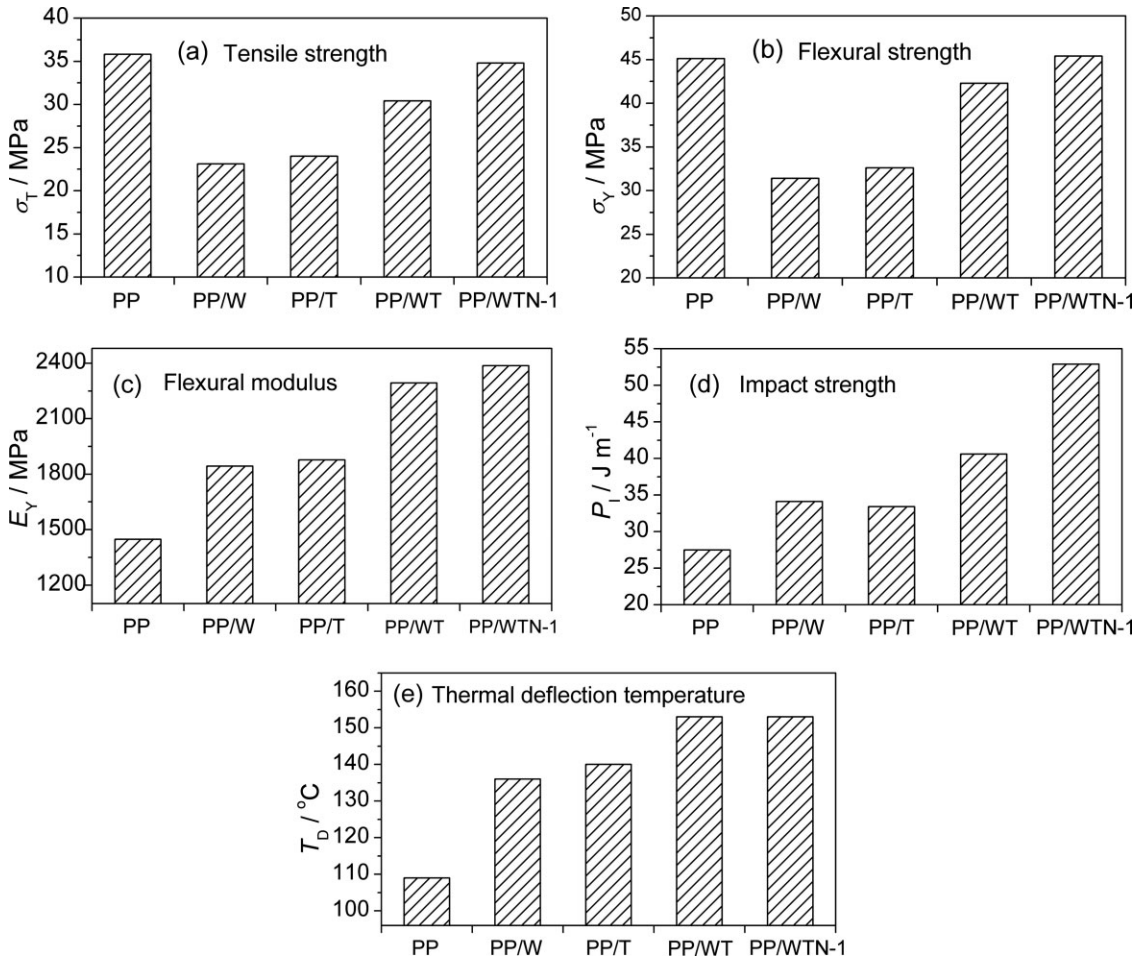

Figure 3 Comparison of the mechanical properties and thermal deflection temperature of PP/W, PP/T, PP/WT, and PP/WTN composites with 35% of inorganic fillers.

show a similar change [Fig. 3(b)]: PP/W ≈ PP/T < PP/WT < PP/WTN-1 ≈ PP matrix.

Figure 3(c) compares the flexural moduli of the composites of PP/W, PP/T, PP/WT, and PP/WTN-1. The flexural moduli of PP/W and PP/T are much higher than that (1447 MPa) of PP matrix, whereas their moduli are lower than that of PP/WT composite. The addition of 0.35% nano-Al_2O_3 further enhance the flexural modulus of PP/WTN-1 (2387 MPa) higher than that of PP/WT. The notched impact strengths of the composites of PP/W, PP/T, PP/WT, and PP/WTN-1 are shown in Figure 3(d). The notched impact strengths of PP/T and PP/W are higher than that of PP matrix, and the PP/WT composite has a high notched impact strength up to 40.6 J/m, which is much larger than that of the PP/T and PP/W composites. For PP/WTN-1 composite, its notched impact strength is as high as 52.9 J/m. Therefore, one can readily conclude that PP matrix << PP/W < PP/T << PP/WT < PP/WTN-1 for flexural moduli and notched impact strengths. As Figure 3(e) shows, inorganic fillers enhance the HDTs of the composites remarkably. The HDT increases from 109°C for PP matrix to 132°C for PP/W and to 140°C for PP/T. The HDTs of PP/WT and PP/WTN-1 composites are up to 153°C, higher than those of PP/W and PP/T composites.

From the above results, we can find that the combination of inorganic particles with various morphologies is in favor of toughening and strengthening of PP composites, and the addition of nanoparticles can toughen and strengthen PP materials simultaneously.

PP/WTN micro-/nanocomposites: the effects of nano-Al_2O_3

Figure 4 shows the mechanical properties and HDTs of the PP/WTN micro-/nanocomposites with 35% of WTN fillers as a function of the mass ratios of nano-Al_2O_3 (N) to WT from 0 to 8%. The tensile strengths of PP/WTN composites linearly increase from 30.4

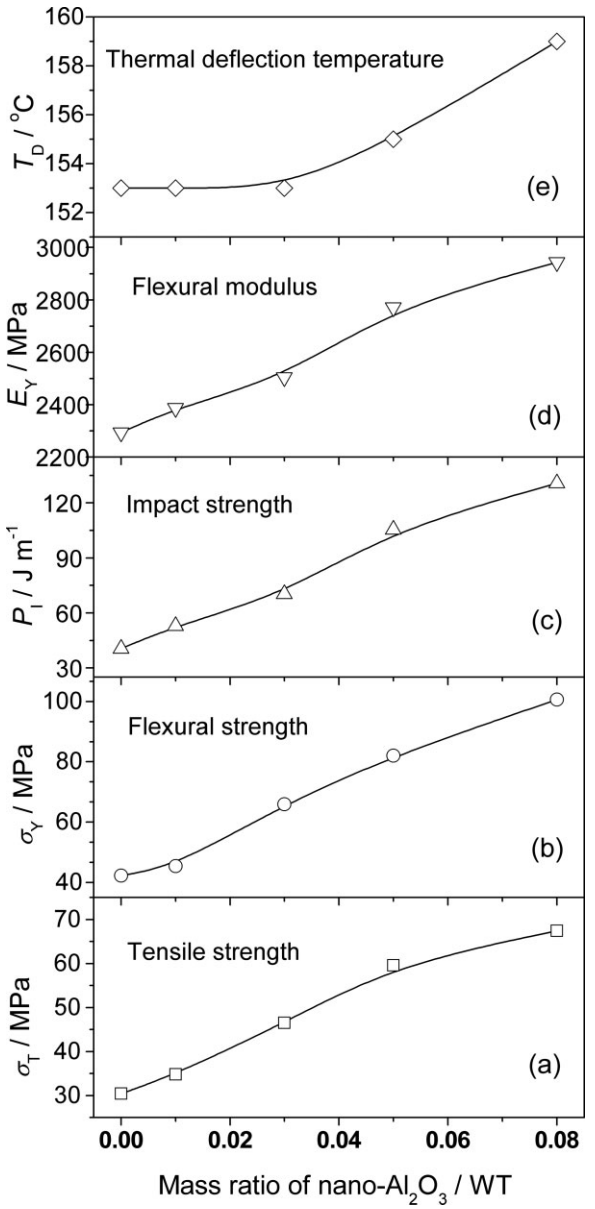

Figure 4 Plots of the mechanical properties and thermal deflection temperature of the PP/WTN micro-/nanocomposites with 35% of WTN as a function of the mass ratio of nano-Al_2O_3 to WT.

MPa for PP/WT to 67.4 MPa for PP/WTN-8, as shown in Figure 4(a). The flexural strengths of the PP/WTN composites, as shown in Figure 4(b), also linearly increase from 42.3 MPa for PP/WT to 100.7 MPa for PP/WTN-8. Similarly, the notched impact strengths of the PP/WTN composites increase from 40.8 J/m for PP/WT to 130.8 J/m for PP/WTN-8, as shown as Figure 4(c), and the flexural moduli increase from 2293 MPa for PP/WT to 2943 MPa for PP/WTN-8 [Fig. 4(d)]. For the HDTs [Fig. 4(e)], the composites of PP/WT, PP/WTN-1, and PP/WT-3 have the same value of 153°C, and with further increases in the nano-Al_2O_3 amount, the HDT increases from 155°C for PP/WT-5 to 159°C for PP/WT-8.

For the PP/WTN-1 composite with 0.35% nano-Al_2O_3, its tensile and flexural strength is very close to that of PP matrix, whereas its flexural modulus, impact strength are much higher than those of PP matrix (Fig. 3). When the amounts of nano-Al_2O_3 used are larger than 0.35%, such as PP/WTN-3, PP/WTN-5, and PP/WTN-8, their strengths, moduli, impact performance, and HDTs are remarkably enhanced when compared with those of PP matrix (Fig. 4). For the PP/WTN-3 composite with 1.0% nano-Al_2O_3, its impact strength, flexural strength, flexural modulus, tensile strength, and HDT are 2.6, 1.5, 1.7, 1.3, and 1.4 times that of PP matrix, respectively. For the PP/WTN-8 composite with 2.59% nano-Al_2O_3, its impact strength, flexural strength, flexural modulus, tensile strength, and HDT are 4.8, 2.2, 2.0, 1.9, and 1.5 times that of PP matrix, respectively.

Dynamic viscosity of PP/CIF melts

The dynamic viscosities of the PP/WT melts with various amounts of WT tested under a frequency of 10 Hz are shown in Table II. As the date show, the dynamic viscosity of the PP/WT melts increases linearly as the amount of WT increases from 20 to 55%. For purposes of comparison, the dynamic viscosity of PP/WTN (65/35) melts with various amounts of nano-Al_2O_3. It can be readily found that the dynamic viscosity of PP/WT melt is much higher than that of pure PP melt by an order of magnitude. But the dynamic viscosity of PP/WTN melts with small amounts (0.35–2.59%) of nano-Al_2O_3 is as low as the similar order of magnitude of the pure PP melt. For

TABLE II
Dynamic Viscosity of PP/WT Melts with Various Fractions of WT, and PP/CIF Melts with 35% of CIFs Measured at a Frequency of 10 Hz

Melt system	Viscosity (η) (Pa s)	Melt system	Viscosity (η) (Pa s)
PP/WT(80/20)	1.63	PP matrix	0.33
PP/WT(70/30)	2.71	PP/WTN-1(65/35)	0.37
PP/WT(65/35)	4.05	PP/WTN-3(65/35)	0.41
PP/WT(60/40)	4.81	PP/WTN-5(65/35)	0.49
PP/WT(55/45)	5.92	PP/WTN-8(65/35)	0.58
PP/WT(45/55)	7.66		

the PP/WTN melts, the viscosity increases with increases in the amounts of nano-Al_2O_3, similar to the literature data.[41] The reduced dynamic viscosity indicates that Al_2O_3 nanocrystals improve the interfacial affinity of WT and PP. The improved interfacial affinity and reduced dynamic viscosity of the PP/WTN systems are in favor of the uniform dispersion of fillers in the PP matrix.

Morphology of the tensile-fractured surfaces of PP/CIF composites

Figure 5 shows typical SEM images of the surfaces of the tensile-fractured surfaces of (a) PP/WT, (b) PP/WTN-1, and (c) PP/WTN-5 composites. As Figure 5(a) shows, there are many bare particles (about 2–5 μm) and cavities on the tensile-fractured surface of the PP/WT composite, whereas for PP/WTN-1, there are few bare particles observed, and the filler particles are seem to be buried into the PP matrix, as shown in Figure 5(b). Figure 5(c) shows that some small particles with diameters less than 1 μm can be found on the tensile-fractured surface of PP/WTN-5, and the drawn particles seem to be enwrapped by PP resin (marked with an ellipse). The dissociated small particles should be the Al_2O_3 nanoparticles enwrapped by PP resin. In addition, obvious transition-layers around the interfaces of inorganic fillers (white regions) with PP matrix (gray regions) are clearly discerned, as the arrows marked in Figure 5(b,c). Some particles debonded from the PP matrix can also be found, such as the particle marked with "A" in Figure 5(b) and the particle marked with "B" in Figure 5(c). The debonding of inorganic filler particles can absorb a large amount of impact energy, which is in favor of toughening. The morphological difference of the tensile-fractured surfaces between PP/WT and PP/WTN indicates that the addition of nano-Al_2O_3 has improved the interfacial adhesion, which results in a remarkable enhancement in mechanical properties, especially in tensile and flexural strengths. The aforementioned result is also supported by the difference in dynamical viscosity of PP/WT and PP/WTN melts.

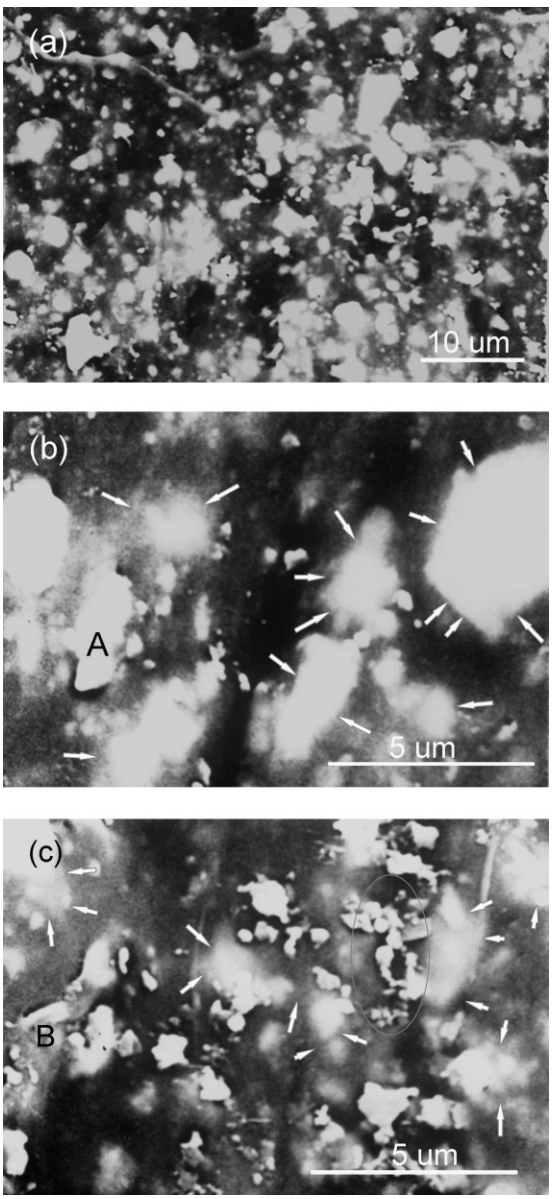

Figure 5 Typical SEM images of the tensile-fractured surfaces of PP/CIFs micro-/nanocomposites with 35% of CIFs: (a) PP/WT, (b) PP/WTN-1, and (c) PP/WTN-5.

Mechanism of synergistic enhancement in mechanical properties

The combinational inorganic filler of WT consisting of plate-like talc powders and needle-like wollastonite powders is more favorable in toughening and strengthening PP than the corresponding singular filler of W or T (Fig. 3). One of the possible reasons can be the synergistic effect of different morphologies of the filler particles of WT.[31,41] Such synergistic effect is probably through an engaging mechanism between plate-like talc particles and needle-like wollastonite particles. The joggled lap joints of talc and wollastonite particles form geometrically stable skeleton structures (e.g., tetrahedral configuration), and PP molecular chains are entangled along the inorganic skeletons, filling in the interspaces in inorganic skeletons and impenetrating through the inorganic skeletons to form a reinforced integrated composite.[38] However, for the filler systems consisting of particles with a singular morphology, the filler particles are commonly difficult to form a skeleton with high geometrical stability, and the fillers usually

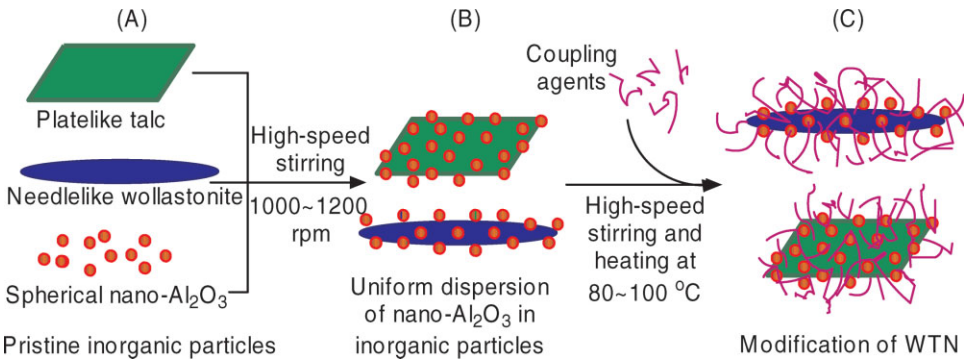

Figure 6 A schematic representation of the uniform dispersion of nano-Al_2O_3 in WTN fillers and their surface modification. [Color figure can be viewed in the online issue, which is available at www.interscience.wiley.com.]

orientate to a certain direction.[17,41] For example, neither talc microplates nor wollastonite microneedles can readily form a geometrically stable skeleton with stereovoids, whereas their mixtures are easy to construct geometrically stable stereovoids under random mixing processes.[17] The synergistic effect of filler morphologies can explain the reason why the mechanical properties of PP/WT composite are much higher than those of PP/W and PP/T composites under the same conditions of materials preparation and testing. We also note that the tensile and flexural strengths of PP/WT composite are lower than those of PP matrix (Figs 2 and 3), which indicates that interfacial adhesion between inorganic fillers and PP matrix is not strong enough. In addition, various inorganic fillers may also influence the crystallization behavior of PP,[31] which then influences the properties of the PP-matrix composites.[13]

Another noticeable experimental result obtained in this work is that the CIFs of WTN with small amounts (0.35–2.59%) of nano-Al_2O_3 can simultaneously strengthen and toughen PP-matrix composites to a large extent (Fig. 4). From the above result we can infer that the PP/WTN composites should have high interfacial adhesion strengths between PP matrix and WTN filler particles, and that the filler particles, especially the Al_2O_3 nanocrystals, have been uniform dispersed in the PP matrix. The following we try to explain how these things happen in the WTN/PP system.

It is well-known that nanocrystals with small sizes have large specific areas and high activity.[41] The Al_2O_3 nanocrystals used in this work are spherical particles with a small size distribution of 10–15 nm and are of unique redispersibility [Fig. 1(c)]. In fact, the used Al_2O_3 nanocrystals are completely fluey. Such well-dispersed Al_2O_3 nanocrystals should have a large specific surface area and can readily be adhered onto the surfaces of the microsized WT particles during the course of high-speed stirring, as shown as the step A→B in Figure 6. By this processing, Al_2O_3 nanocrystals can be uniformly dispersed in the mixture of talc and wollastonite powders. As the coupling agents are added to the mixture of WT and nano-Al_2O_3 under a heating (80–100°C) and stirring (1000–1200 rpm) condition, the molecular chains of the coupling agents ought to be preferentially adsorbed onto the nano-Al_2O_3 particles which have adhered to the surfaces of WT powders via chemical/physical interaction forces. This process can be illustrated as the step B→C in Figure 6. The surfaces of the WTN modified with coupling agents, therefore, become very hydrophobic, and similar to the physiochemical characteristics of the PP resin. In addition, the active nano-Al_2O_3 particles, without enough covering chains of coupling agents, can interact with PP chains intensively to form a thick transition layer between inorganic filler particles and PP matrix through a strong chemical adsorption or physical tanglement. The thick transition layers reduce the viscosity of the PP/CIF melts, and the reduced viscosity is in favor of the uniform dispersion of the WTN particles. It should be noted that this thick transition layer is different from the core/shell encapsulation structure by an elastomers phase.[28] On the other hand, the thick transition layer between inorganic WTN particles and PP matrix is helpful to enhance the interfacial adhesion strength,[17] which results in the enhanced tensile and flexural strengths of the PP/WTN composites. These inferences have been supported by the mechanical properties [Figs. (3 and 4)], microstructures of the tensile-fractured surfaces (Fig. 5), and the results of dynamical viscosity (Table II).

The addition of CIFs with micrometric and nanoscale particles should also have an synergistic effect in improving the crystallization of PP matrix and refining their grains,[13,31,42,50] which then results in the enhancement of the mechanical properties of PP/CIF composites. Also, the mechanical ultrafine

grinding in the course of the preparation of CIFs is helpful to enhance the activity of inorganic particles and the enhanced activity of inorganic particles then to improve the interfacial adhesion of CIF/PP,[13,17] which facilitates the reinforcements of the PP-matrix composites.

CONCLUSIONS

We have developed an effective route to reinforce PP-matrix composites using CIFs, consisting of micrometric talc, micrometric wollastonite, and nanoscale Al_2O_3 particles as the reinforcement components via an extrusion and injection molding process. The combinational fillers (WT) consisting talc and wollastonite were more favorable in reinforcing PP-matrix composites than the fillers consisting of singular species of inorganic particles (i.e., W or T). The combinational fillers (WTN) with small amounts of nanoscale Al_2O_3 particles simultaneously strengthened and toughened the PP-matrix composites by a remarkable enhancement in tensile strength, flexural strength and modulus, notched impact strength, and HDT, when compared with the PP/WT or PP matrix. The simultaneous strengthening and toughening of PP-matrix composites were attributed to the synergistic effects of the CIFs, not only because of the synergistic effects of various morphologies (plate-like, needle-like and spherical) of the inorganic particles but also because of the synergistic effects of hierarchical dimensions (microscale and nanoscale) of inorganic particles. The artful combination of conventional micrometric inorganic fillers and nanocrystals not only have overcome the limitations of reducing tensile/flexural strengths in conventional inorganic-rigid-particle modification of polymers but also have successfully solved the puzzle how to disperse nanocrystals in a polymer matrix uniformly using a simple process. This route proposed is robust, cost-effective and advanced, and is feasible for industrialization. The technique can be extended to reinforce other polymer systems with some modification.

References

1. Park, S. Y.;Park, E. J.; Lee, M. Y.; Park, C.; Kim, H. G.; Jeong, E. D.; Lim, K. T. Polym Adv Technol 2008, 19, 1803.
2. Miroslavá, M.; Mravčákova, M.; Chodák, I.; Pionteck, J.; Häussler, L. Polym Eng Sci 2006, 46, 1069.
3. Reddy, C. S.; Das, C. K.; Narkis, M. Polym Compos 2005, 26, 806.
4. Costache, M. C.; Wang, D.; Heidecker, M. J.; Manias, E.; Wilkie, C. A. Polym Adv Technol 2006, 17, 272.
5. Karian, H. G. Handbook of Polypropylene and Polypropylene Composites; Marcel Dekker: New York, 2003.
6. Bonner, M.; Ward, I. M.; Mcgregor, W.; Tanner, K. E.; Bonfield, W. J. Mater Sci Lett 2001, 20, 2049.
7. Yang, J. P.; Yang, G.; Xu, G. S.; Fu, S. Y. Compos Sci Technol 2007, 67, 2934.
8. Albano, C.; Papa, J.; Ichazo, M.; Gonzalez, J.; Ustariz, C. Compos Struct 2003, 62, 291.
9. Najafi, S. K.; Kiaefar, A.; Tajvidi, M. J Appl Polym Sci 2008, 110, 3116.
10. Montoya, M.; Abad, M. J.; Barral Losada, L.; Bernal, C. J Appl Polym Sci 2005, 98, 1271.
11. Miyazaki, K.; Moriya, K.; Okazaki, N.; Terano, M.; Nakatani, H. J Appl Polym Sci 2009, 111, 1835.
12. Qi, D.; Shao, J.; Wu, M.; Nitta, K. Front Chem Eng China 2008, 2, 396.
13. Wang, T.; Liu, D.; Keddie, J. L. J Appl Polym Sci 2007, 106, 386.
14. Xia, H.; Wang, Q.; Li, K.; Hu, G.-H. J Appl Polym Sci 2004, 93, 378.
15. Zhu, P.; Chen, J.; Wu, C. Polym Compos 2008, DOI 10.1002/pc.20566.
16. Li, Y.; Wang, S.; Zhang, Y.; Zhang, Y. J Appl Polym Sci 2006, 102, 104.
17. Chen, M.; Wan, C.; Shou, W.; Zhang, Y.; Zhang, Y.; Zhang, J. J Appl Polym Sci 2008, 107, 1718.
18. Chen, X.; Yu, J.; Guo, S.; Luo, Z.; He, M. Polym Compos 2009, 30, 941.
19. Boudenne, A.; Ibos, L.; Fois, M.; Gehin, E.; Majeste, J.-C. J Polym Sci Part B: Polym Phys 2004, 42, 722.
20. Shen, J.; Ji, G.; Hu, B.; Huang, Y. J Mater Sci Lett 1993, 12, 1344.
21. Shelesh-Nezhad, K.; Taghizadeh, A. Polym Eng Sci 2007, 47, 2124.
22. Lazzeri, A.; Thio, Y. S.; Cohen, R. E. J Appl Polym Sci 2004, 91, 925.
23. Wang, S.; Xu, W.; Zhou, Z.; Ren, F. J Appl Polym Sci 2009, 111, 532.
24. Chen, D.; Zhang, H.; Zheng, Q.; Liu, F.; Xu, K.; Chen, M. Polym Adv Technol 2008, 19, 1353.
25. Lee, S. H.; Zhang, Z. X.; Xu, D.; Chung, D.; Oh, G. J.; Kim, J. K. Polym Eng Sci 2009, 49, 168.
26. Zhou, Z.; Cui, L.; Zhang, Y.; Zhang, Y.; Yin, N. J Polym Sci Part B: Polym Phys 2008, 46, 1762.
27. Zhou, Z.; Zhang, Y.; Zeng, Z.; Zhang, Y. J Appl Polym Sci 2008, 110, 3745.
28. Premphetha, K.; Preechachon, I. J Appl Polym Sci 2003, 89, 3557.
29. Li, Z.; Guo, S.; Song, W.; Yan, Y. Polym Sci Part B: Polym Phys 2002, 40, 1804.
30. Wang, X.; Sun, J.; Huang, R. J Appl Polym Sci 2006, 99, 2268.
31. Švab, I.; Musil, V.; Jurkin, T.; Šmit, I. Polym Eng Sci 2007, 47, 2145.
32. Yu, J.; Wang, G.; Chen, J.; Zeng, X.; Wang, W. Polym Eng Sci 2007, 47, 201.
33. González-Sánchez, C.; González-Quesada, M.; Orden, M. U.; Urreaga, J. M. J Appl Polym Sci 2008, 110, 2555.
34. Bouza, R.; Abad, M. J.; Barral, L.; Ladra, M. Polym Eng Sci 2009, 49, 324.
35. Panthapulakkal, S.; Sain, M. J Polym Environ 2006, 14, 265.
36. Zhang, S.; Rodrigue, D.; Riedl, B. Polym Compos 2005, 26, 731.
37. Mirbagheri, J.; Tajvidi, M.; Hermanson, J. C.; Ghasemi, I. J Appl Polym Sci 2007, 105, 3054.
38. Zhang, M. Q.; Rong, M. Z.; Zeng, H. M.; Schmitt, S.; Wetzel, B.; Friedrich, K. J Appl Polym Sci 2001, 80, 2218.
39. Jin, S. H.; Kang, C. H.; Yoon, K. H.; Bang, D. S.; Park, Y.-B. J Appl Polym Sci 2009, 111, 1028.
40. Joo, J. H.; Shim, J. H.; Choi, J. H.; Choi, C.-H.; Kim, D.-S.; Yoon, J.-S. J Appl Polym Sci 2008, 109, 3645.

41. Mishra, S.; Sonawane, S.; Mukherji, A.; Mruthyunjaya, H. C. J Appl Polym Sci 2006, 100, 4190.
42. Mishra, S.; Sonawane, S. H.; Singh, R. P. J Polym Sci Part B: Polym Phys 2005, 43, 107.
43. Erdem, N.; Cireli, A. A.; Erdogan, U. H. J Appl Polym Sci 2009, 111, 2085.
44. Zhu, Y.; Xu, Y.; Tong, L.; Xu, Z.; Fang, Z. J Appl Polym Sci 2008, 110, 3130.
45. Rong, M. Z.; Zhang, M. Q.; Pan, S. L.; Friedrich, K. J Appl Polym Sci 2004, 92, 1771.
46. Tarapow, J. A.; Bernal, C. R.; Alvarez, V. A. J Appl Polym Sci 2009, 111, 768.
47. Song, P.; Tong, L.; Fang, Z. J Appl Polym Sci 2008, 110, 616.
48. Xu, N.; Zhou, W.; Shi, W. Polym Adv Technol 2004, 15, 654.
49. Vaisman, L.; Marom, G.; Wagner, H. D. Adv Funct Mater 2006, 16, 357.
50. Khosh, R. L.; Bagheri, R.; Zokaei, S. J Appl Polym Sci 2008, 110, 4040.
51. Saujanya, C.; Radhakrishanan, S. J Mater Sci 2000, 35, 2319.
52. Chen, D. L.; Yang, H. M.; Gao, L. Mater Sci Eng (Chinese) 2003, 19, 220.
53. Chen, X.; Wu, H.; Luo, Z.; Yang, B.; Guo, S.; Yu, J. Polym Eng Sci 2007, 47, 1756.
54. Liang, J.-Z. J Appl Polym Sci 2007, 104, 1697.